

# Defect characterization by differential capacitance spectroscopy without the Arrhenius plot

Cite as: Rev. Sci. Instrum. 92, 043903 (2021); doi: 10.1063/5.0047128

Submitted: 10 February 2021 • Accepted: 20 March 2021 •

Published Online: 1 April 2021



View Online



Export Citation



CrossMark

Jian V. Li<sup>a</sup> 

## AFFILIATIONS

Department of Aeronautics and Astronautics, National Cheng Kung University, Tainan 701, Taiwan

<sup>a</sup>Author to whom correspondence should be addressed: [jianvli@ncku.edu.tw](mailto:jianvli@ncku.edu.tw)

## ABSTRACT

A new method of Arrhenius transformation and matching is developed in this study based on the rate-temperature duality of the admittance spectroscopy measurement to extract the activation energy  $E_a$  and the attempt-to-escape frequency  $v_0$  of a defect in GaAsN from differential capacitance spectroscopy without the Arrhenius plot and without identifying the  $f\partial C/\partial f$  spectra peaks. The method consists of a set of variations that transform the iso-rate scan and/or the isothermal scan to a virtual space—activation energy, attempt-to-escape frequency, temperature, or rate. The transformed scans must be matched prior to extracting  $E_a$  and  $v_0$  local to a fixed point in the two-dimensional temperature-rate experimental space.

Published under license by AIP Publishing. <https://doi.org/10.1063/5.0047128>

Carrier emission from defects<sup>1,2</sup> in semiconductor materials is a thermally activated process.<sup>3</sup> The admittance spectroscopy (AS)<sup>4,5</sup> finds defects by identifying a peak in the frequency differential capacitance  $f\partial C/\partial f$  spectra at a certain temperature and frequency  $f_{peak}$ ; the latter is related to the carrier emission/capture rate<sup>1</sup> by  $f_{peak} = v/2\pi$ . According to the Arrhenius equation,

$$v = v_0 \exp(-E_a/k_B T), \quad (1)$$

where  $E_a$  is the activation energy of the defect,  $v_0$  is the attempt-to-escape frequency,  $k_B$  is Boltzmann's constant, and  $T$  is temperature. The measurements of  $E_a$  and  $v_0$  are essential to the characterization of defects, and such measurements have traditionally relied on the classic Arrhenius plot line-fitting (APL) method.<sup>1</sup> Over a range of temperatures,  $E_a$  is extracted from the slope and  $v_0$  is extracted from the y-intercept by line-fitting the Arrhenius plot that is composed of the peak frequencies of the  $f\partial C/\partial f$  spectra.

The APL method requires accurate identification of the peak positions in the  $f\partial C/\partial f$  spectra and cannot extract  $E_a$  and  $v_0$  local to a temperature point, which contain valuable information of a non-Arrhenius process.<sup>6,7</sup> Recently, I developed the Arrhenius transformation and matching (ATM) method to extract  $E_a$  and  $v_0$  without identifying the peaks and therefore bypassing

the Arrhenius plot from deep-level transient spectroscopy<sup>8</sup> and capacitance-frequency<sup>9</sup> measurement (a rare form of AS). In this work, I systematically present the ATM method for extracting  $E_a$  and  $v_0$  from the differential capacitance  $f\partial C/\partial f$  spectra (the standard<sup>5</sup> form of AS).

The admittance measurement was performed with a Keysight 4294A impedance analyzer from 100 Hz to 1 MHz with 35 mV<sub>rms</sub> AC modulation voltage. The sample was a  $1 \times 1 \text{ mm}^2$  GaAs<sub>0.988</sub>N<sub>0.012</sub> asymmetrical PN<sup>+</sup> junction (p-doping =  $1.38 \times 10^{17} \text{ cm}^{-3}$ ) solar cell<sup>10</sup> grown by metal-organic chemical vapor deposition. The temperature of the sample was stabilized between 12 and 450 K in a Janis closed-cycle He-cooled cryostat.

Figure 1 shows the  $f\partial C/\partial f$  contour plot in the temperature-rate plane with two defects. This work focuses on defect 1 only, which has a larger  $f\partial C/\partial f$ . The APL method uses the locus of the peaks in the  $T-v$  space (the black solid line in Fig. 1) to construct the Arrhenius plot (data not shown). Then,  $E_a = 335 \pm 1 \text{ meV}$  and  $\log_{10}(v_0) = 13.4 \pm 0.1 \text{ s}^{-1}$  are extracted from the plot by line-fitting between 160 and 240 K.

By rearranging the Arrhenius equation [Eq. (1)], one can obtain the various Arrhenius transformations between the spaces of the two experimentally controllable parameters ( $T$  and  $v$ ) and the two parameters to be extracted ( $E_a$  and  $v_0$ ) as follows:

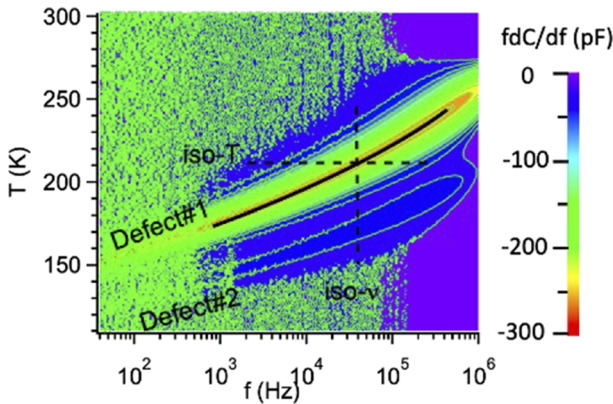


**FIG. 1.** The contour plot of  $fdC/df$  in the  $T$ - $\nu$  plane. The isothermal and iso-rate scans at any ( $T_{fix}$ ,  $\nu_{fix}$ ) point (examples in dashed lines) may be visualized as “slicing” through the  $fdC/df$  surface in the 2D  $T$ - $\nu$  space. This contour plot is constructed from 220 pre-transformation  $fdC/df$  vs  $f$  spectra with a temperature step size of 1.0 K and 301 frequency points in each spectrum.

$T$ - $E_a$  transformation:

$$E_{a,T} = k_B T \ln(\nu_0 / \nu_{fix}), \quad (2)$$

$\nu$ - $E_a$  transformation:

$$E_{a,\nu} = k_B T_{fix} \ln(\nu_0 / \nu), \quad (3)$$

$T$ - $\nu_0$  transformation:

$$\nu_{0,T} = \nu_{fix} \exp(E_a / k_B T), \quad (4)$$

$\nu$ - $\nu_0$  transformation:

$$\nu_{0,\nu} = \nu \exp(E_a / k_B T_{fix}), \quad (5)$$

$T$ - $\nu$  transformation:

$$\nu_T = \nu_{fix} \times \exp[E_a / k_B \times (T^{-1} - T_{fix}^{-1})], \quad (6)$$

$\nu$ - $T$  transformation:

$$T_\nu = T_{fix} \times [\ln(\nu_0) - \ln(\nu)] / [\ln(\nu_0) - \ln(\nu_{fix})], \quad (7)$$

where  $\nu_{fix}$  and  $T_{fix}$  are from a fixed point in the  $T$ - $\nu$  space and all other parameters on the LHS of the equations are transformed parameters.

Consider the two independent scans indicated by the dashed lines in Fig. 1: (i) the iso-rate scan  $fdC/df(T)$  with fixed  $\nu_{fix}$  and (ii) the isothermal scan  $fdC/df(v)$  with fixed  $T_{fix}$ . One can use Eq. (2) to turn  $fdC/df(T)$  into a virtual scan  $fdC/df(E_{a,T})$ , accomplishing a  $T$ - $E_a$  transformation in the  $E_a$  space. Similarly, one can use Eq. (3) to transform  $fdC/df(v)$  into a virtual scan  $fdC/df(E_{a,v})$ . The  $T$ - $E_a$  and  $\nu$ - $E_a$  transformations share the same  $\nu_0$ , which adjusts simultaneously the curvatures of  $fdC/df(E_{a,T})$  and  $fdC/df(E_{a,v})$ . Both experimental scans,  $fdC/df(v)$  and  $fdC/df(T)$ , are based on the same thermally activated process that determines the carrier exchange rate. Therefore, the necessary and sufficient condition for two corresponding virtual scans  $fdC/df(E_{a,v})$  and  $fdC/df(E_{a,T})$  to concur is to

use the  $\nu_0$  in the  $T$ - $E_a$  and  $\nu$ - $E_a$  transformations from the thermal activation process from which these scans were physically obtained. Once  $\nu_0$  is determined,  $E_a$  can then be calculated through Eq. (1) at  $(T_{fix}, \nu_{fix})$ . Alternatively,  $E_a$  can be read from the common peak shared by  $fdC/df(E_{a,v})$  and  $fdC/df(E_{a,T})$ . Figure 2(a) is an example of applying this procedure to extract  $\log_{10}(\nu_0) = 13.1 \text{ s}^{-1}$  and calculate  $E_a = 338 \text{ meV}$  local to  $T_{fix} = 197 \text{ K}$ . These results agree well with what the APL method produces. In the exaggerated cases of  $\log_{10}(\nu_0) = 12.9 \text{ s}^{-1}$  and  $13.3 \text{ s}^{-1}$ , the matching is poor. Similarly, one can use Eqs. (4) and (5) to transform  $T/\nu$  to  $\nu_0$  space, obtain the best fit value of  $E_a$  by matching the virtual scans, and calculate  $\nu_0$  from Eq. (1). While the fixed point  $(\nu_{fix}, T_{fix})$  can be any arbitrary point in the  $T$ - $\nu$  plane in principle, the points near the solid line in Fig. 1 are the more convenient choices because the curvatures match at the peak of two  $fdC/df$  spectra and the near-peak data are less noisy.

Alternatively, one can use Eq. (6) to perform a  $T$ - $\nu$  transformation and generate a virtual scan  $fdC/df(\nu_T)$  from an experimental iso-rate scan  $fdC/df(T)$ , which is matched to the experimental isothermal scan  $fdC/df(v)$ ; to obtain the best fit value of  $E_a$ ; and to calculate  $\nu_0$ . Figure 2(b) is an example of applying the

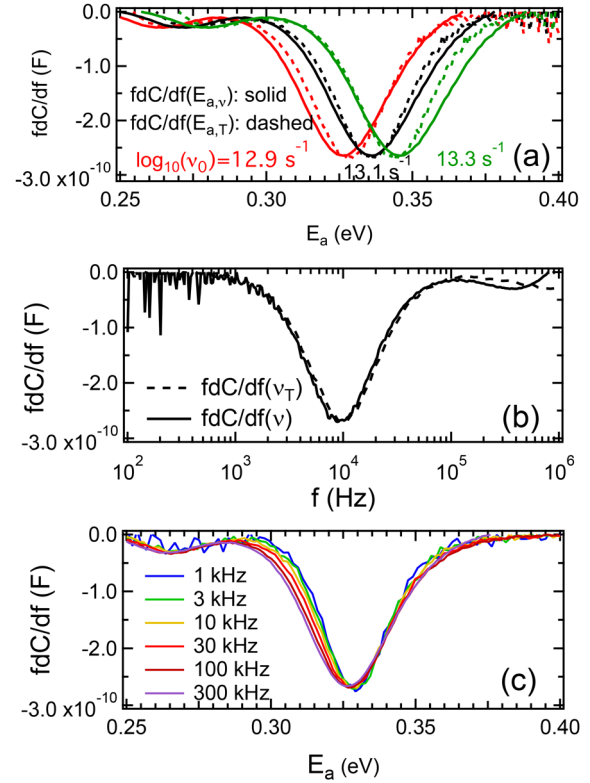


**FIG. 2.** (a) The virtual scan  $fdC/df(E_{a,v})$  (solid) and iso-rate scan  $fdC/df(E_{a,T})$  (dashed) are transformed from the isothermal ( $T_{fix} = 197 \text{ K}$ ) and iso-rate ( $\nu_{fix} = 10 \text{ kHz}$ ) scans using Eqs. (2) and (3). A match (black) is obtained with  $\log_{10}(\nu_0) = 13.1 \text{ s}^{-1}$ . Green and red curves show exaggerated poor matching. (b) The virtual scan  $fdC/df(v)$  (dashed) is transformed from the experimental iso-rate ( $\nu_{fix} = 10 \text{ kHz}$ ) scan  $fdC/df(v)$  (solid) to extract  $E_a = 338 \text{ meV}$ . (c) Several iso-rate  $fdC/df(T)$  scans are transformed to the  $E_a$  space using Eq. (2) with  $\log_{10}(\nu_0) = 13.1 \text{ s}^{-1}$ . The resultant  $fdC/df(E_{a,T})$  spectra collapse together.

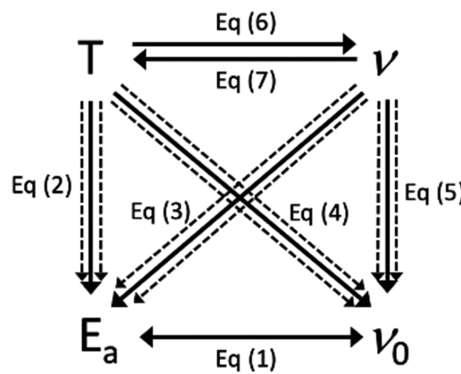


**FIG. 3.** A diagram summarizing the variations of the ATM method. The transformations between  $T$ ,  $v$ ,  $E_a$ , and  $v_0$ , which are based on the Arrhenius equation indicated by the double-ended arrow, are represented by single-ended arrows with the corresponding equations labeled next to them.

above-mentioned procedure to extract  $E_a = 338$  meV and calculate  $\log_{10}(v_0) = 13.1\text{ s}^{-1}$  from Eq. (1). A symmetrical variation of the ATM method<sup>11</sup> based on the temperature-rate duality<sup>12</sup> uses Eq. (7) to perform the  $v-T$  transformation and generate a virtual scan  $f\text{d}C/\text{d}f(T_v)$  from an experimental isothermal scan  $f\text{d}C/\text{d}f(v)$ , which is matched to the experimental isothermal scan  $f\text{d}C/\text{d}f(T)$  to obtain the best fit value of  $v_0$  and calculate  $E_a$ .

In practical situations, only one kind of scan, either iso-rate or isothermal, may be preferred as the other may be unavailable or sparsely distributed in the  $T-v$  space. In this case, one can use one of Eqs. (2)–(5) to transform all scans of that particular kind (iso-rate or isothermal) to either the  $E_a$  or the  $v_0$  virtual space. Figure 2(c) is an example of how all the iso-rate  $f\text{d}C/\text{d}f(T)$  scans taken at several temperatures are transformed to the  $E_a$  space using only Eq. (2). All resultant virtual scans  $f\text{d}C/\text{d}f(E_{a,T})$  collapse together, indicative of an optimal fitting condition for extracting  $\log_{10}(v_0) = 13.1\text{ s}^{-1}$  used in Eq. (2). Since  $T_{fix}$  is not defined in this case,  $E_a$  cannot be calculated from Eq. (1). Instead,  $E_a = 328$  meV is read directly from the shared peak of all  $f\text{d}C/\text{d}f(E_{a,T})$  spectra.

Figure 3 is a summary of all the variations of the ATM method. The three types of transformation and matching between  $T$ ,  $v$ ,  $E_a$ , and  $v_0$  are represented by arrows with the corresponding equations labeled next to them. (i) As in the example in Fig. 2(a), transformation involving two single-ended solid arrows [Eqs. (2)–(5)] are required to match one isothermal to one iso-rate scan in the  $E_a/v_0$  virtual space. (ii) Only one transformation involving one of the two single-ended solid arrows between  $T$  and  $v$  [Eqs. (6) and (7)] is

needed to match the virtual scan to another experimental scan, as shown in Fig. 2(b). (iii) The dashed arrows pointing from  $T/v$  to  $E_a/v_0$  indicate that one of these four transformations [Eqs. (2)–(5)] can be used to transform and collapse multiple spectra of the same kind, as shown in Fig. 2(c). After the best fit value of either  $E_a$  or  $v_0$  is determined from one of the three scenarios mentioned above, the other parameter is calculated from Eq. (1) at  $(T_{fix}, v_{fix})$  as indicated by the double-ended arrow or simply read from the common peak shared by the virtual scans.

In conclusion, the ATM method from the differential capacitance spectroscopy is demonstrated to extract  $E_a$  and  $v_0$  without using the Arrhenius plot and without identifying the peaks in the  $f\text{d}C/\text{d}f$  spectra. This method extends Arrhenius equations to transform the experimental isothermal and iso-rate scans to the activation energy, attempt-to-escape frequency, temperature, or rate virtual space and extracts  $E_a$  and  $v_0$  at any temperature point by matching the curvatures of the virtual scans and the experimental scans.

The author thanks Dr. S. Kurtz and Dr. S. W. Johnston from National Renewable Energy Laboratory, USA, for providing the GaAsN sample and sharing the AS technique. This research was supported, in part, by the Ministry of Science and Technology, Taiwan, under Grant No. MOST-107-2218-E-006-022-MY3.

## DATA AVAILABILITY

The data that support the findings of this study are available from the corresponding author upon reasonable request.

## REFERENCES

- <sup>1</sup>P. Blood and J. W. Orton, *The Electrical Characterization of Semiconductors: Majority Carriers and Electron States* (Academic Press, London, 1992).
- <sup>2</sup>C. T. Sah, *Fundamentals of Solid-State Electronics* (World Press, Singapore, 1990).
- <sup>3</sup>S. Arrhenius, *Z. Phys. Chem.* **4**, 226 (1889).
- <sup>4</sup>D. L. Losee, *J. Appl. Phys.* **46**, 2204 (1975).
- <sup>5</sup>T. Walter *et al.*, *J. Appl. Phys.* **80**, 4411 (1996).
- <sup>6</sup>D. V. Lang *et al.*, *Appl. Phys. Lett.* **50**, 736 (1987).
- <sup>7</sup>D. Wickramaratne *et al.*, *Appl. Phys. Lett.* **113**, 192106 (2018).
- <sup>8</sup>J. V. Li, *Rev. Sci. Instrum.* **92**, 023902 (2021).
- <sup>9</sup>J. V. Li, *J. Phys. Chem. C* **125**, 2860 (2021).
- <sup>10</sup>S. W. Johnston and S. R. Kurtz, *J. Vac. Sci. Technol. A* **24**, 1252 (2006).
- <sup>11</sup>J. V. Li, S. W. Johnston, Y. Yan, and D. H. Levi, *Rev. Sci. Instrum.* **81**, 033910 (2010).
- <sup>12</sup>S. Agarwal, Y. N. Mohapatra, and V. A. Singh, *J. Appl. Phys.* **77**, 3155 (1995).